Pseudolaric acid B induces apoptosis associated with the mitochondrial and PI3K/AKT/mTOR pathways in triple-negative breast cancer

KE YANG[1*], JUN-QI WANG[2*], KAI LI[3], SU-NING CHEN[1] and FEI YU[1]

Departments of [1]Traditional Chinese Medicine, [2]General Surgery and [3]Oncology, Shengjing Hospital of China Medical University, Shenyang, Liaoning 110004, P.R. China

Received May 18, 2023; Accepted August 18, 2023

DOI: 10.3892/or.2023.8630

Abstract. Pseudolaric acid B (PAB), a diterpene acid isolated from the root bark of *Pseudolarix kaempferi*, has been shown to exert strong antitumor properties. The aim of the present study was to investigate the mechanisms underlying the proposed antitumor properties of PAB in the triple-negative breast cancer cells, MDA-MB-231. The cell processes evaluated included cell proliferation by Cell Counting Kit-8 assay, colony formation and EdU assay, apoptosis by Annexin V-FITC/PI apoptosis assay, cell migration by Transwell migration assay and invasion by Transwell invasion assay. PAB significantly inhibited the proliferation of MDA-MB-231 cells through a mechanism that was considered to be associated with cell cycle arrest at the G_2/M phase. There was decreased protein expression levels of CDK1 and cyclin B1 and increased protein expression levels of p53 and p21. However, there were no well-defined inhibitory effects on the normal breast cell line MCF10A. PAB also triggered apoptosis in a concentration-dependent manner through the mitochondrial apoptosis pathway. It caused collapse of mitochondrial membrane potential, accumulation of reactive oxygen species and release of cytochrome c, as well as upregulation of cleaved caspase-3, cleaved caspase-9, cleaved PARP and Bax, and downregulation of Bcl-2 and Bcl-xl. The migration and invasion ability of MDA-MB-231 cells were inhibited by decreasing the expression levels of the epithelial-mesenchymal transition-related markers N-cadherin and vimentin and increasing the expression of E-cadherin. Moreover, the expression levels of PI3K (p110β), phosphorylated (p)-AKT (ser^{473}) and p-mTOR (ser^{2448}) were downregulated and LY294002, a PI3K inhibitor, could interact additively with PAB to induce apoptosis of MDA-MB-231 cells. Overall, the present results demonstrated that PAB induced apoptosis via mitochondrial apoptosis and the PI3K/AKT/mTOR pathway in triple-negative breast cancer. It also inhibited cellular proliferation, migration and invasion, suggesting that PAB may be a useful phytomedicine for the treatment of triple-negative breast cancer.

Correspondence to: Professor Fei Yu, Department of Traditional Chinese Medicine, Shengjing Hospital of China Medical University, 36 Sanhao Street, Heping, Shenyang, Liaoning 110004, P.R. China
E-mail: yuf1@sj-hospital.org

*Contributed equally

Key words: pseudolaric acid B, apoptosis, migration, invasion, mitochondrial PI3K/AKT/mTOR

Introduction

According to global cancer statistics published by the International Agency for Research on Cancer of the World Health Organization, breast cancer surpassed lung cancer in 2020 to become the most diagnosed cancer in the world (1). Triple-negative breast cancer (TNBC) is the most aggressive subtype of breast cancer, characterized by negative expression of estrogen receptor, progesterone receptor and human epidermal growth factor receptor-2 (2). Although this subtype accounts for 15-20% of all types of breast cancer, it lacks effective therapeutic targets and treatment options are limited (3). Therefore, it is critical to find novel therapeutic targets for the treatment of TNBC.

Pseudolaric acid B (PAB) is a diterpene acid derived from the cortex of *Pseudolarix kaempferia* (golden larch) that exhibits diverse properties, including anti-inflammatory (4), antifungal (5), antiangiogenic (6), pro-apoptotic (7) and microtubule-destabilizing (8) effects. In previous years, researchers have shown that PAB has antitumor effects in liver cancer (9), gastric cancer (10), medulloblastoma (7), lung cancer (11) and leukemia (12). However, the mechanisms underlying these antitumor effects remain unclear.

Apoptosis, also known as programmed cell death, is a form of self-cleaning in which the body removes damaged cells in an orderly and efficient manner. The dysregulation of apoptosis is a major reason for the unlimited proliferation exhibited by tumor cells (13). Thus, dysregulation of apoptosis is considered one of the hallmarks of cancer. The mitochondrial apoptotic pathway comprises the core apoptotic signaling pathway in vertebrates and is triggered by a change in mitochondrial outer membrane permeabilization (14). Subsequently, cytochrome c is released from the mitochondria into the cytoplasm,

stimulating caspase-3 and other mechanisms of apoptosis (15). Previous studies demonstrated that PAB induces apoptosis through the mitochondrial and death receptor pathway in numerous types of cancer, including hepatocellular (9), cervical (16), head and neck (17) and colorectal cancer (18). However, to the best of our knowledge, the apoptotic mechanism of PAB in TNBC has not been studied.

The PI3K/AKT/mTOR signaling pathway plays a key role in several processes of tumor development, such as apoptosis, proliferation, metabolism and metastasis (19). It can also enhance the malignancy of various types of tumor cells (20). Previous studies have demonstrated that PI3K/AKT/mTOR signaling affects the mitochondrial apoptosis pathway by regulating proteins in the Bcl-2 family (21-23).

The present study aimed to explore the anticancer activity and related mechanisms of PAB in the TNBC MDA-MB-231 cell line. Effects of PAB on migration and invasion were also investigated.

Materials and methods

Reagents and antibodies. PAB was purchased from Beijing Solarbio Science & Technology Co., Ltd. Primary antibodies for caspase-3 (1:1,000; cat. no. 19677-1-AP), caspase-9 (1:1,000; cat. no. 10380-1-AP), Bax (1:2,000; cat. no. 50599-2-Ig), Bcl-2 (1:2,000; cat. no. 60178-1-Ig), p53 (1:5,000; cat. no. 80077-1-RR), p21 (1:2,000; cat. no. 10355-1-AP) and GAPDH (1:8,000; cat. no. 10494-1-AP), and HRP-conjugated Affinipure goat anti-rabbit (cat. no. SA00001-2; 1:8,000) and anti-mouse (cat. no. SA00001-1; 1:8,000) IgG secondary antibodies were purchased from ProteinTech Group, Inc. In addition, the primary antibodies for PARP (cat. no. T40050); Bcl-xl (cat. no. T40057), Cytochrome c (cat. no. T55734), PI3K (cat. no. T55224), AKT (cat. no. T55561), p-AKT (cat. no. T40067), mTOR (cat. no. T55306), p-mTOR (cat. no. T56571) (all 1:1,000) were purchased from Abmart Pharmaceutical Technology Co., Ltd. Antibodies for CDK1 (1:1,000; cat. no. PTM-6521), cyclin B1 (1:1,000; cat. no. PTM6659), Vimentin (1:1,000; cat. no. PTM5376), E-cadherin (1:2,000; cat. no. PTM6222) and N-cadherin (1:1,000; cat. no. PTM5221) were purchased from PTM Biolabs, Inc. Annexin V-FITC/PI Apoptosis Detection kit was purchased from Vazyme Biotech Co., Ltd. Cell Counting Kit-8 (CCK-8) was purchased from MedChemExpress. Mitochondrial membrane potential (MMP) assay kit with JC-1 (cat. no. C2006) and western stripping buffer (cat. no. P0025N) were purchased from Beyotime Institute of Biotechnology.

Cell culture. The TNBC cell line MDA-MB-231 and human breast cell line MCF-10A were donated by the Department of Oncology, Shengjing Hospital of China Medical University (Shenyang, China). MDA-MB-231 cells were cultured in Leibovitz's L-15 medium (Procell Life Science & Technology Co., Ltd.) containing 5% fetal bovine serum (FBS; Procell Life Science & Technology Co., Ltd.) and 1% antibiotics (100 U/ml penicillin and 100 U/ml streptomycin). MCF10A cells were cultured in DMEM/F12 (Procell Life Science & Technology Co., Ltd.) containing 5% HS, 20 ng/ml epidermal growth factor, 0.5 μg/ml Hydrocortisone, 10 μg/ml insulin, 1% non-essential amino acid and 1% antibiotics (100 U/ml penicillin and 100 U/ml streptomycin). MDA-MB-231 cells were grown free of CO_2 in a cell culture incubator at 37˚C. MCF-10A cells were cultured at 37˚C with 5% CO_2.

Cell viability assay. The effect of PAB on cellular viability was measured using a CCK-8 assay. Cells ($5x10^3$/well) were cultured in a 96-well plate overnight, then treated with different concentrations of PAB (0, 2.5, 5, 7.5, 10, 12.5 and 15 μM) at 37˚C for 24, 48 and 72 h. After treatment, the medium was removed and a mixture of 90 μl medium (Leibovitz's L-15 or DMEM/F12) and 10 μl CCK-8 reagent was added to each well (24). After 2 h of incubation at 37˚C, the absorbance at 450 nm was measured using a microplate reader.

Colony formation assay. To explore the effect of PAB on cellular proliferation, the colony formation assay was conducted. MDA-MB-231 and MCF-10A cells ($1x10^3$/well) were seeded in six-well plates overnight, then treated with different concentrations of PAB (5, 7.5 and 10 μM) at 37˚C for 48 h before changing back to a drug-free medium (Leibovitz's L-15 or DMEM/F12). Cells were cultured for an additional 14 days, then fixed with 4% polyoxymethylene at room temperature for 15 min and stained with 0.1% crystal violet at room temperature for 15 min. After removing the crystal violet, plates were washed twice with phosphate-buffered saline (PBS) and the number of colonies was counted and analyzed by Image J 1.8.0 software (National Institutes of Health). A colony with more than 50 cells is defined as a colony.

EdU staining assay. The BeyoClick™ EdU-488 cell proliferation kit (Beyotime Institute of Biotechnology) was used to evaluate the effect of PAB on cellular proliferation. MDA-MB-231 cells ($2x10^4$/well) were seeded in 12-well plates and cultured at 37˚C overnight. The kit was used according to manufacturer's instructions. Briefly, cells were incubated with medium containing EdU (10 μM) at 37˚C for 2 h, then fixed with 4% paraformaldehyde for 15 min at room temperature. Cells were then stained with the Click reaction solution at room temperature for 30 min in darkness. Next, cell nuclei were stained using Hoechst 33342 and images were captured using a fluorescence microscope (Nikon Corporation) at a magnification of 100.

Cell cycle analysis. Cells were treated with 5, 7.5 and 10 μM PAB at 37˚C for 48 h. After harvesting and washing with pre-cold PBS, cells ($1x10^6$/ml) were resuspended with cold 70% ethanol and fixed at 4˚C overnight. Cells were washed twice with PBS and centrifuged at 1,000 x g at 4˚C for 5 min to remove residual ethanol, then stained with 50 μg/ml propidium iodide (PI) and 100 μg/ml RNase solution (Beijing Solarbio Science & Technology Co., Ltd.) at 37˚C for 20 min (25). The cell cycle arrest in G_2-M phase was measured using flow cytometry (FACS Calibur; BD Biosciences) and analyzed with FlowJo 7.6 software (FlowJo LLC).

Apoptosis assay. The rate of apoptosis was detected using the annexin V-FITC/PI apoptosis kit (Vazyme Biotech Co., Ltd.) according to the manufacturer's instructions. Briefly, MDA-MB-231 cells ($2x10^5$) were seeded in six-well plates overnight, then cultured with PAB (5, 7.5 and 10 μM),

LY294002 (40 μM) or both (7.5 μM PAB + 40 μM LY294002) at 37˚C for 48 h. Next, cells were harvested with EDTA-free trypsin and washed twice with chilled PBS. Cell precipitates were resuspended with 1X binding buffer and then stained with 5 μl annexin V-FITC and 5 μl PI staining solution in the dark for 10 min at room temperature (24,26). Finally, the rate of apoptosis was analyzed by flow cytometry (FACS Calibur; BD Biosciences).

Assessment of MMP and (reactive oxygen species) ROS. Considering that a decline in MMP is a key trigger to activate the mitochondrial apoptosis pathway, MMP assay kit with JC-1 was used to detect the MMP level of MDA-MB-231 cells. JC-1 forms aggregates in the mitochondrial matrix when the MMP is high, resulting in red fluorescence. When the MMP is low, JC-1 cannot aggregate in the mitochondrial matrix and cells fluoresce is green. Briefly, after treatment with PAB (5, 7.5 and 10 μM) at 37˚C for 48 h, cells were harvested and resuspended in 500 μl JC-1 working solution, in the darkness at 37˚C for 20 min. Cells were then washed twice with chilled JC-1 staining buffer (1X) and immediately examined using flow cytometry (FACS Calibur; BD Biosciences).

To assess ROS levels, cells were cultured with PAB (5, 7.5 and 10 μM) at 37˚C for 48 h, then collected and incubated with 10 μM DCFH-DA fluorescent probe for 20 min at 37˚C in the darkness. The cells were washed twice with FBS-free Leibovitz's L-15 medium (Procell Life Science & Technology Co., Ltd.) and the cellular ROS level was detected using flow cytometry (FACS Calibur; BD Biosciences).

DAPI staining. Cells ($1x10^4$/well) were seeded on glass coverslips in 24-well plates overnight, then treated with PAB (5, 7.5 and 10 μM) at 37˚C for 48 h. The cells were fixed with 4% paraformaldehyde at room temperature for 15 min and permeabilized with 0.5% Triton X-100 at room temperature for 20 min. After washing three times with PBS, the cells were stained with fluorescent dye DAPI in a darkroom at room temperature for 15 min. The nuclear morphology was observed using a fluorescence microscope at a magnification of 200.

Transwell migration and invasion assays. Cell migration and invasion assays were performed using Transwell chambers with a pore size of 8 μm (27). Matrigel (Corning Biocoat; Corning Life Sciences) was used for the cell invasion assay but not for the cell migration assay. A mixture of Martrigel and FBS-free Leibovitz's L-15 medium was added to the upper chamber and placed at 37˚C for 1 h. Cells were cultured with serum-free Leibovitz's L-15 medium overnight, then suspended and diluted to a density of $1x10^5$ with various concentrations of PAB (5, 7.5 and 10 μM). A 200 μl cell suspension containing $2x10^4$ cells was added to the upper chamber on the 24-well plate. The lower chamber was filled with 500 μl Leibovitz's L-15 medium supplemented with 10% FBS. After incubation at 37˚C for 48 h, the cells that passed through the chambers were fixed with 4% paraformaldehyde at room temperature for 20 min, stained with 0.1% crystal violet at room temperature for 30 min and then non-penetrating cells were wiped off with a cotton swab. Cells were observed under light microscope at a magnification of 100.

Wound healing assays. MDA-MB-231 cells were grown in six-well plates until the cell confluence reached 100%. A wound was made by scratching the adherent cell layer with a 200-μl pipette tip (25). Shed cells were washed off with PBS and the remaining cells were treated with serum-free Leibovitz's L-15 medium containing different concentrations of PAB (5, 7.5 and 10 μM) for 48 h. Cells were observed under light microscope at a magnification of 200. Data analysis was performed using ImageJ 1.8.0 software (National Institutes of Health). The rate of wound healing=[(the wound width of 0-48 h)/0 h wound width] x100%.

Western blotting. Protein expression levels were evaluated using western blotting as previously described (26,28). Cells were treated with 5, 7.5 and 10 μM PAB at 37˚C for 48 h, then lysed with RIPA buffer (Beyotime Institute of Biotechnology) for protein extraction. Cells were centrifuged at 10,000 x g for 15 min at 4˚C, and protein concentrations were measured using a BCA Protein Assay kit (Beyotime Institute of Biotechnology). Protein samples (30 μg/lane) were separated using 10-12.5% SDS-PAGE gels before being transferred to the PVDF membrane (MilliporeSigma). PVDF membranes were horizontally cut to probe proteins with different molecular weights. After blocking with 5% skim milk diluted with Tris-buffered saline with Tween (TBST) containing 0.1% Tween at room temperature for 2 h, the PVDF membranes were incubated with primary antibodies at 4˚C overnight. Blots were washed three times with TBST and incubated with secondary antibodies for 2 h at room temperature. Stripping buffer was used to remove the antigen-antibody complex from the PVDF membrane in order to re-probe other antibodies on the same membrane. The blots were measured using SuperFemto ECL Chemiluminescence kit (Vazyme Biotech Co., Ltd) through the chemiluminescence detection system of the Amersham Imager 600 (GE Healthcare Production).

Statistical analysis. All data were obtained from three independently replicated experiments and presented as mean ± standard deviation. One-way analysis of variance was used to analyze statistical significance for multiple comparisons, followed by Tukey's multiple comparisons test. $P<0.05$ was considered to indicate a statistically significant difference.

Results

PAB inhibits the proliferation of TNBC cells. To investigate the effect of PAB on the viability of TNBC cells, the CCK-8 assay was performed to evaluate the influence of various concentrations of PAB for 24, 48 and 72 h. PAB inhibited the proliferation of MDA-MB-231 cells in dose- and time-dependent manners, with IC50 values of 19.3, 8.3 and 5.76 μM at 24, 48 and 72 h respectively (Fig. 1A). However, the result of CCK-8 showed that PAB had no obvious side-effects on normal cells line MCF10A (Fig. 1B). Colony formation assays further confirmed that PAB suppressed the proliferation of MDA-MB-231 cells in a dose-dependent manner, but not MCF10A cells (Fig. 1C-F). Furthermore, according to the EdU assay, compared with the control, all three different concentrations (5, 7.5 and 10 μM) of PAB can significantly reduce the number of EDU positive MDA-MB-231 cells (Fig. 2A),

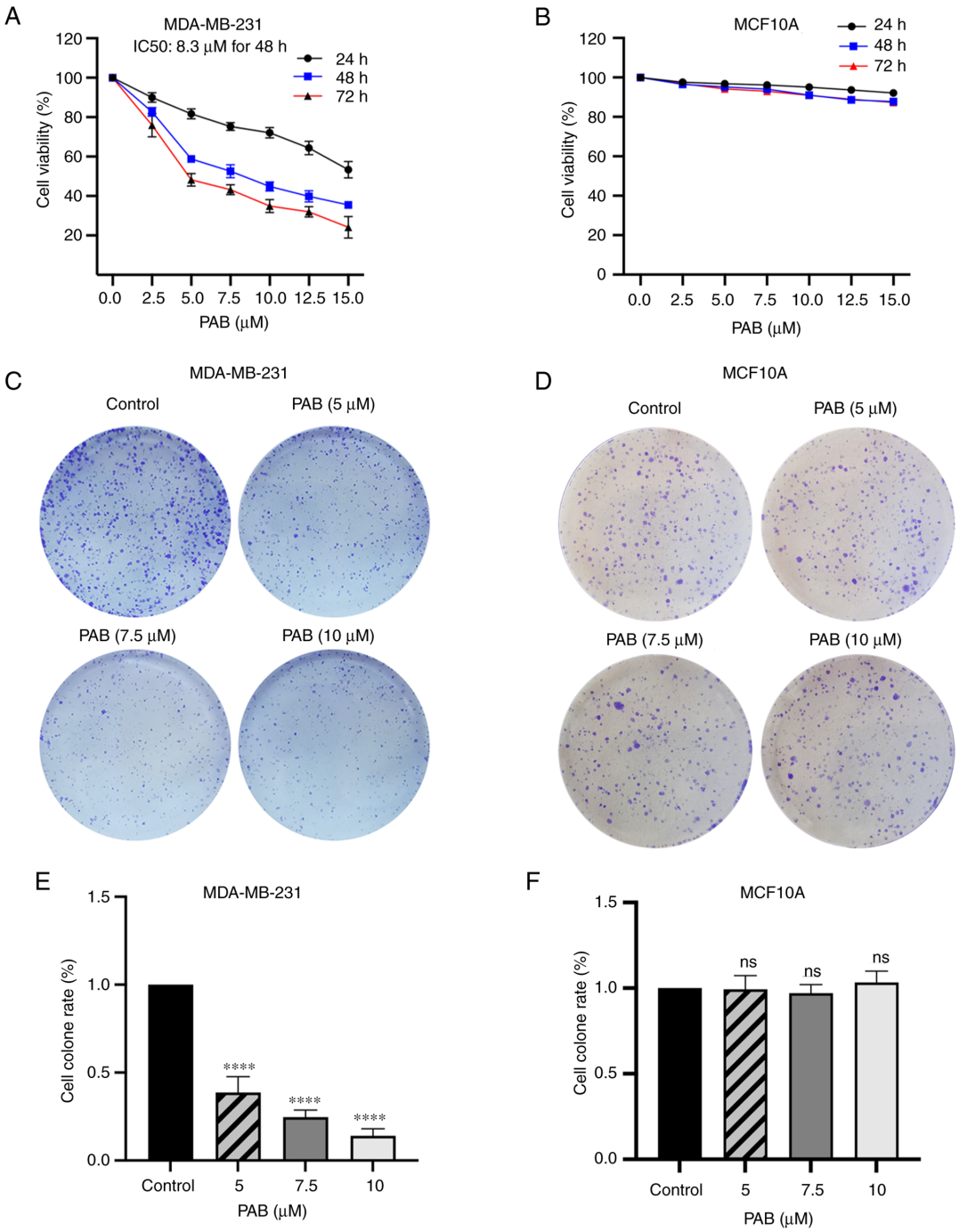

Figure 1. PAB inhibits the growth of MDA-MB-231 cell. (A) MDA-MB-231 and (B) MCF10A cells were incubated with various concentration of PAB for 24, 48 and 72 h, and cell viability was determined using CCK-8 assay. Results of colony formation assays of (C) MDA-MB-231 and (D) MCF10A cells. Quantification of (E) MDA-MB-231 and (F) MCF10A cell colony formation assays. ****P<0.0001 vs. control. CCK-8, Cell Counting Kit-8; PAB, Pseudolaric acid B; ns, not significant.

indicating that PAB could suppress the proliferative capacity of these cells (Fig. 2B).

G_2/M cell cycle arrest of MDA-MB-231 cells is induced by PAB. The cell cycle distribution was analyzed by flow cytometry after propidium iodide staining. MDA-MB-231 cells treated with various concentration of PAB for 48 h were harvested for cell cycle analysis. As shown in Fig. 2C and D, it induced a significant increase in the number of cells in G_2/M phase. Meanwhile, western blotting showed that the protein expression levels of CDK1 and cyclin B1 were significantly reduced compared with the control, while those of p53 and p21 were increased after PAB treatment (Fig. 2E and F). These results indicate that PAB may induce cell cycle arrest by altering the expression of cell recycle regulators.

PAB induces apoptosis via the mitochondrial pathway. After treatment with various concentration of PAB for 48 h, flow cytometry showed that PAB induced apoptosis in MDA-MB-231 cells in a dose-dependent manner (Fig. 3A and B). The effect

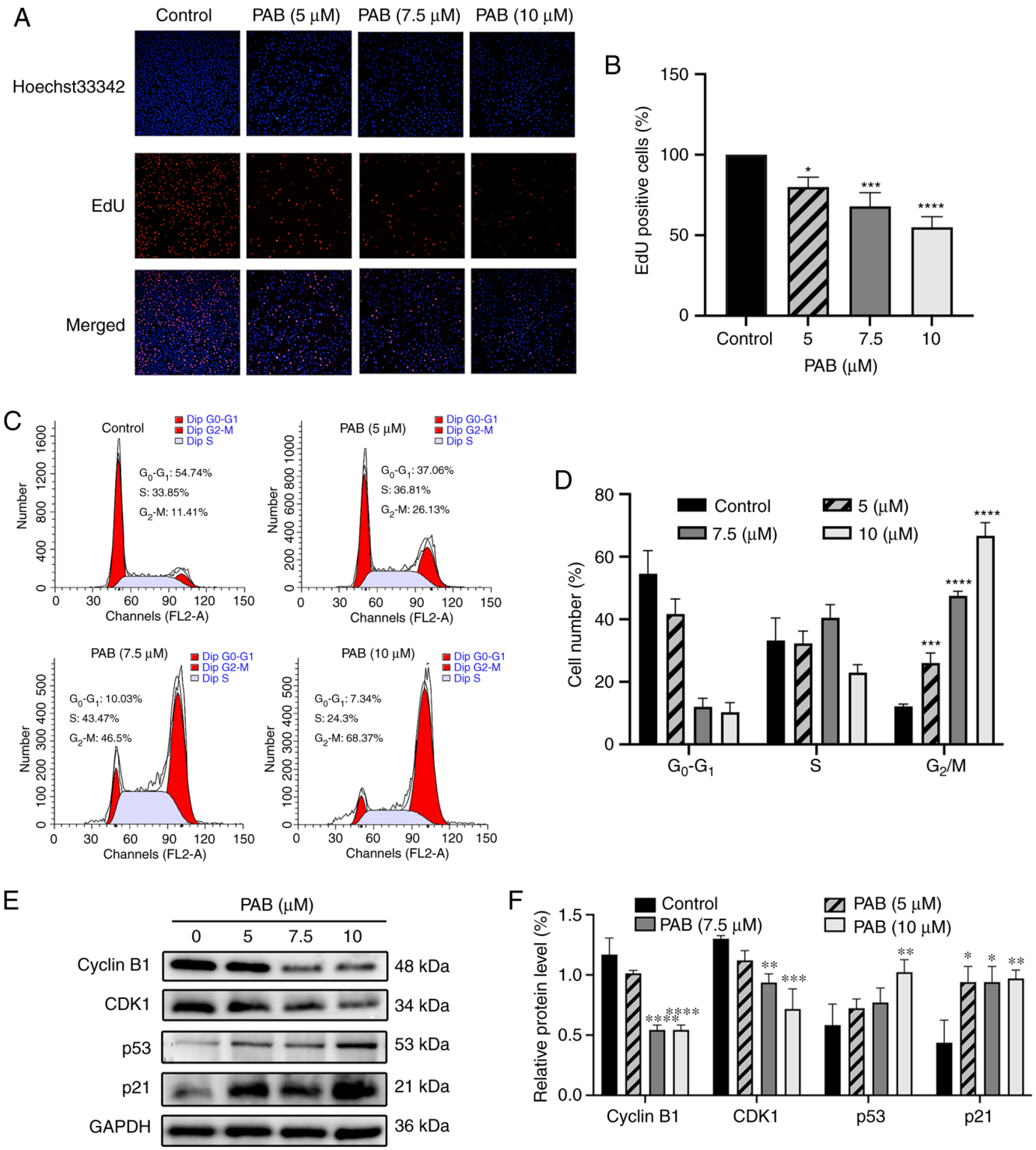

Figure 2. PAB induces cell arrest at the G_2/M phase. (A) MDA-MB-231 cell proliferation was assessed using an EdU assay (magnification, x100). (B) Quantification of the proportion of EdU-positive cells induced by PAB (C) Percentage of cells in G_0-G_1, G_2-M and S phase in MDA-MB-231 cells with or without the treatment of PAB for 48 h. (D) Quantitative data of PAB-induced cell cycle distribution. (E) Western blotting showed Cyclin B1 and CDK1 were inhibited by PAB. p53 and p21 expression are both enhanced as PAB concentration increased. (F) Quantitative data of the relative protein expression. *P<0.05, **P<0.01, ***P<0.001 and ****P<0.0001 vs. control. PAB, Pseudolaric acid B.

of PAB on the nuclear status of MDA-MB-231 cells was tested using DAPI staining. Apoptotic cells presented with nuclear condensation and DNA fragmentation (Fig. 3C).

A collapse of MMP is an important factor leading to apoptosis mediated by the mitochondrial apoptosis pathway. JC-1 staining showed that PAB induced a dose-dependent loss of MMP in MDA-MB-231 cells (Fig. 3D and E). To further explore the mechanisms of PAB-induced apoptosis, the related protein expression was measured and it was revealed that PAB significantly induced Cytochrome c release from the mitochondria into the cytosol (Fig. 4A and B), upregulated the expression of cleaved-caspase3, cleaved-caspase9,

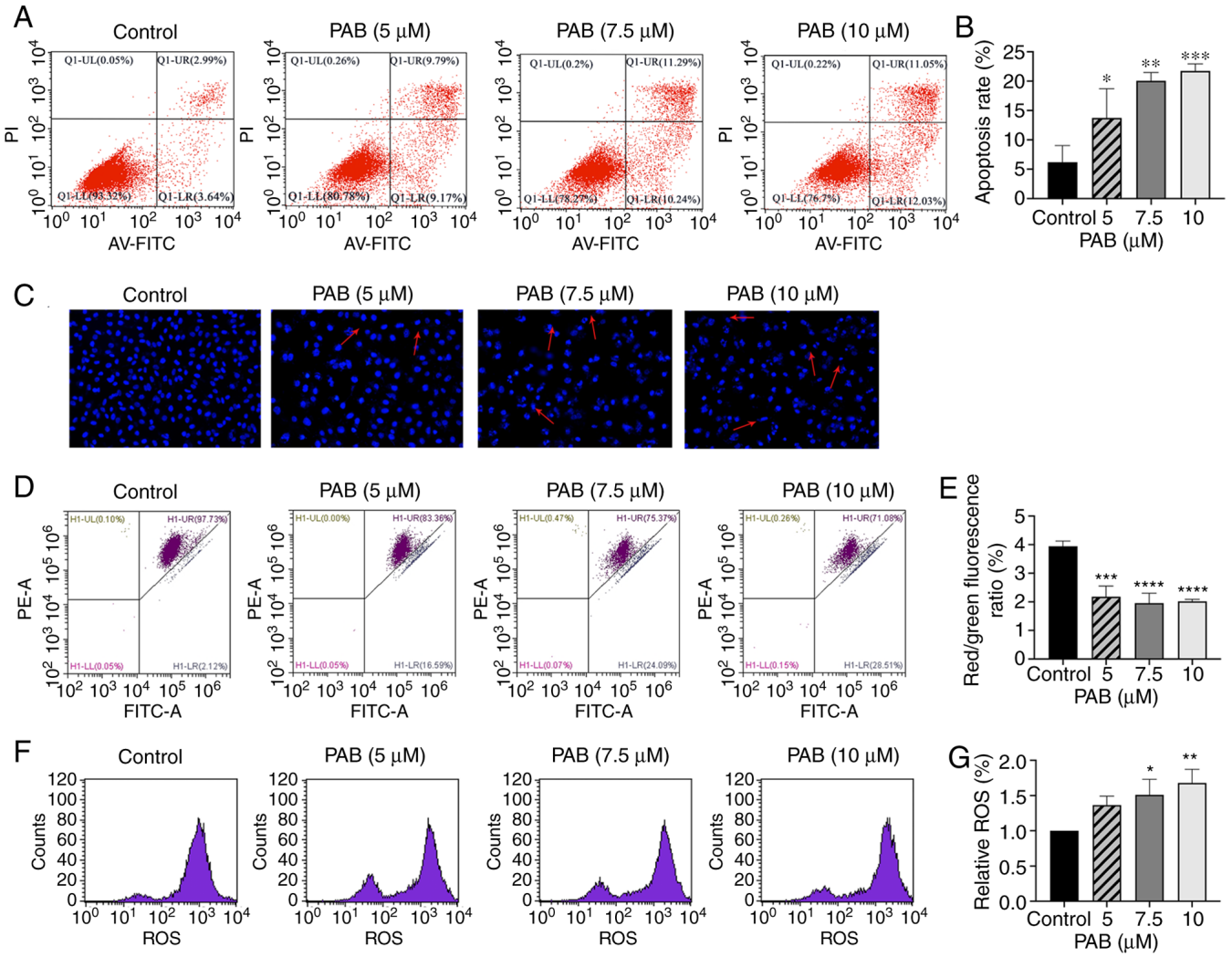

Figure 3. PAB induces apoptosis in MDA-MB-231 cells. (A) Cells were pretreated with PAB (5, 7.5, 10 μM) for 48 h. Annexin V-FITC and PI staining were used to identify the apoptosis, and the data were analyzed by flow cytometry. (B) Quantitative data of PAB-induced apoptosis. (C) Cell nuclei were observed by confocal microscope (magnification, 400x) after 48 h of PAB treatment by DAPI staining. Typical apoptosis morphological changes were shown in treated cells including chromatin condensation and DNA fragmentation. (D) Cell mitochondrial membrane potential was determined using flow cytometry with JC-1 staining after 48 h of treatment with 0, 5, 7.5 and 10 μM PAB, respectively. (E) Red/green fluorescence ratio. The ratio of red to green fluorescence represents the percentage of decreased MMP. (F) Fluorescence in the cell is represented as the percentage of ROS production (G) analyzed using flow cytometry. *P<0.05, **P<0.01, ***P<0.001, ****P<0.0001 vs. control. PAB, Pseudolaric acid B; MMP, mitochondrial membrane potential; ROS, reactive oxygen species.

cleaved-PARP and Bax, and downregulated the expression of Bcl-2 and Bcl-xl (Fig. 4C and D). All these changes were statistically significant (P<0.05). Therefore, the results demonstrated that PAB induced apoptosis mediated by mitochondrial apoptosis pathway in TNBC.

PAB increases ROS levels. It is well known that ROS production is related to mitochondrial pathway-associated apoptosis. Therefore, ROS production was detected by the fluorescent probe DCFH-DA. As shown in Fig. 3F and G, flow cytometry demonstrated that the ROS accumulation was directly related to PAB concentration.

PAB inhibits migration and invasion by regulating the epithelial-mesenchymal transition (EMT) pathway. Migration of MDA-MB-231 cells was measured by the wound healing and Transwell migration assays. PAB significantly inhibited wound healing ability (Fig. 5A and B) and Transwell migration ability (Fig. 5C and D) in a dose-dependent manner. As shown in Fig. 5E and F, PAB significantly inhibited cell invasion. Protein levels of N-cadherin and vimentin were reduced by PAB, while the protein level of E-cadherin was increased (Fig. 5G and H). Overall, these data suggested that PAB inhibited migration, invasion and EMT in MDA-MB-231 cells.

PAB inhibits the PI3K/AKT/mTOR signaling pathway. To investigate the role of the PI3K/AKT/mTOR signaling pathway in the anticancer effect of PAB on MDA-MB-231 cells, the activation of PI3K, AKT and mTOR were evaluated by western blotting. PAB inhibited PI3K (p110β), the phosphorylation of AKT and the phosphorylation of mTOR in a dose-dependent manner and PAB did not influence total levels of AKT and mTOR (Fig. 6A and B). Furthermore, the apoptotic rate of PAB and LY294002 co-treated cells exceeded that of PAB or LY294002 alone (Fig. 6C and D). These results suggested that the PI3K/AKT/mTOR signaling

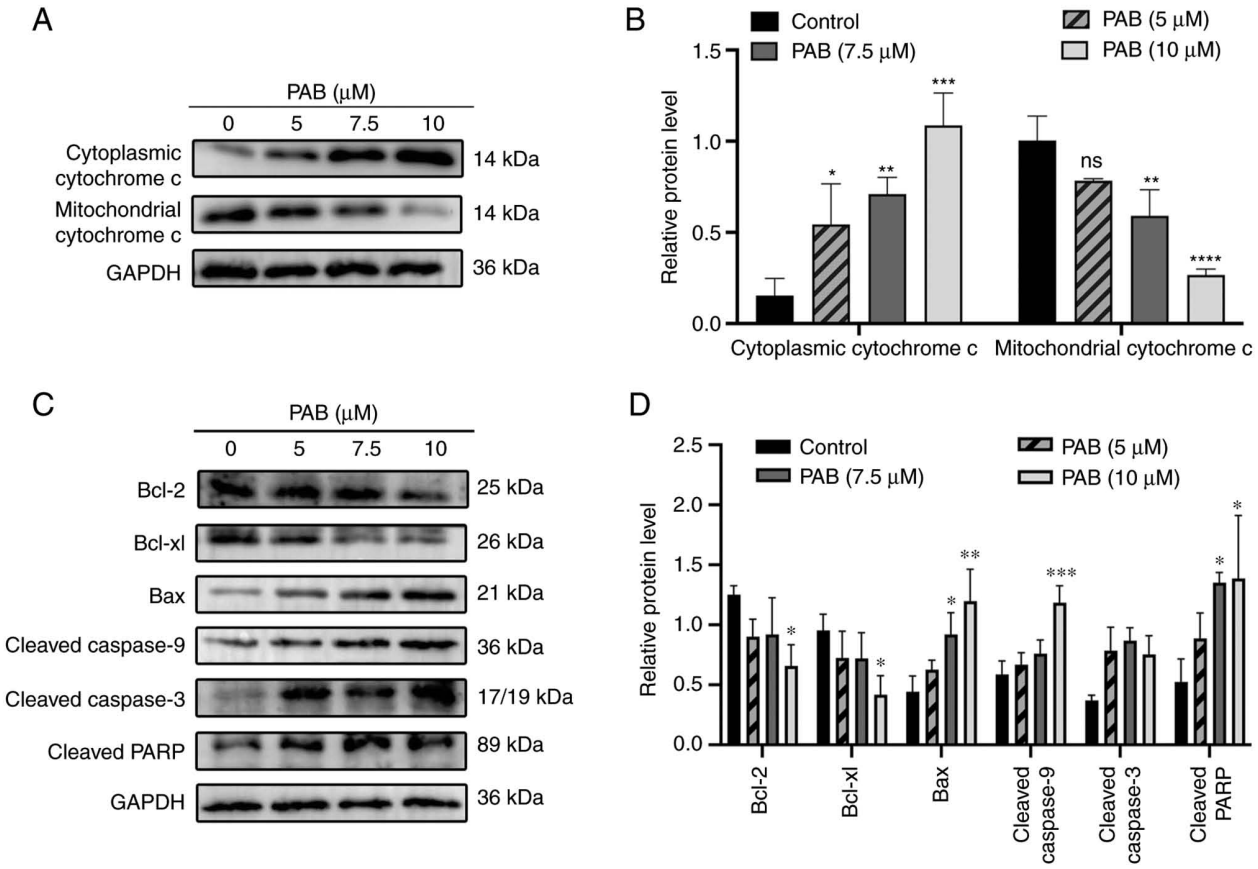

Figure 4. Effect of PAB on mitochondria-mediated apoptotic pathway. (A) PAB significantly induced Cytochrome c released from mitochondria into the cytosol. (B) Quantitative data of the protein expression of Cytochrome c. (C) Western blotting analysis result of the expression levels of Bcl-2, Bcl-xl, Bax, cleaved caspase-9, cleaved caspase-3 and cleaved PARP. (D) Quantitative data of the relative protein expression. *P<0.05, **P<0.01, ***P<0.001, ****P<0.0001 vs. control. PAB, Pseudolaric acid B.

pathway was involved in PAB-induced apoptosis in MDA-MB-231 cells.

Discussion

PAB, the main medicinal component of *Cortex pseudolaricis*, is a natural plant product with potential antifungal, immunosuppressive and anticancer properties. Previous studies have shown that PAB has multi-target anticancer effects in different types of tumors (9,29-31). To investigate the anticancer properties and mechanisms of PAB on TNBC, the present study investigated the effects of PAB on the proliferation, apoptosis, invasion and migration of MDA-MB-231 cells. CCK-8, EdU and colony formation assays demonstrated that PAB inhibited the proliferation of MDA-MB-231 cells in a dose- and time-dependent manner.

Excessive cell division is an important reason for the continuous proliferation of tumor cells (32). Recently, researchers have indicated that numerous natural drugs exert their anticancer effects by regulating the cycle checkpoints, which can lead to arrest of the tumor cell cycle (33-36). Among these checkpoints, cyclin B1 and CDK1 are necessary for the cell cycle to switch from the S to the G_2/M phase (37). The tumor suppressor p53 induces G_2/M phase arrest by activating the downstream transcriptional target p21, which is a CDK inhibitor (38,39). The present results indicated that PAB induced G_2/M phase arrest of MDA-MB-231 cells by upregulating the expression of p53 and p21, resulting in the downregulation of cyclin B1 and CDK1 proteins.

Flow cytometry showed that PAB induced apoptosis in MDA-MB-231 cells in a concentration-dependent manner. Mitochondria are the hubs for cellular energy metabolism, and mitochondrial dysfunction is the main cause for activation of the mitochondrial apoptosis pathway (40). ROS are mainly produced in mitochondria, and its excessive accumulation can damage mitochondria and activate the mitochondria-mediated intrinsic apoptotic pathway (41). To further investigate the mechanism of apoptosis, nuclear morphology, MMP level, ROS levels and protein expression were evaluated. DAPI nuclear staining indicated that PAB led to chromatin condensation, cellular shrinkage and DNA fragmentation. It also caused a decrease of MMP and an increase of ROS. Furthermore, western blotting showed that it upregulated the proapoptotic protein Bax and downregulated the antiapoptotic proteins Bcl-2 and Bcl-xl. Cytochrome c is released from mitochondria into the cytosol and subsequently activates caspase-9 and caspase-3, which help to initiate the mitochondrial apoptosis pathway (42). The present experiments showed that PAB could promote the release of cytochrome c from mitochondria into the cytoplasm. In addition, levels of cleaved caspase-3 and caspase-9, as well as PARP, were increased. Western blotting further demonstrated that it could downregulate the

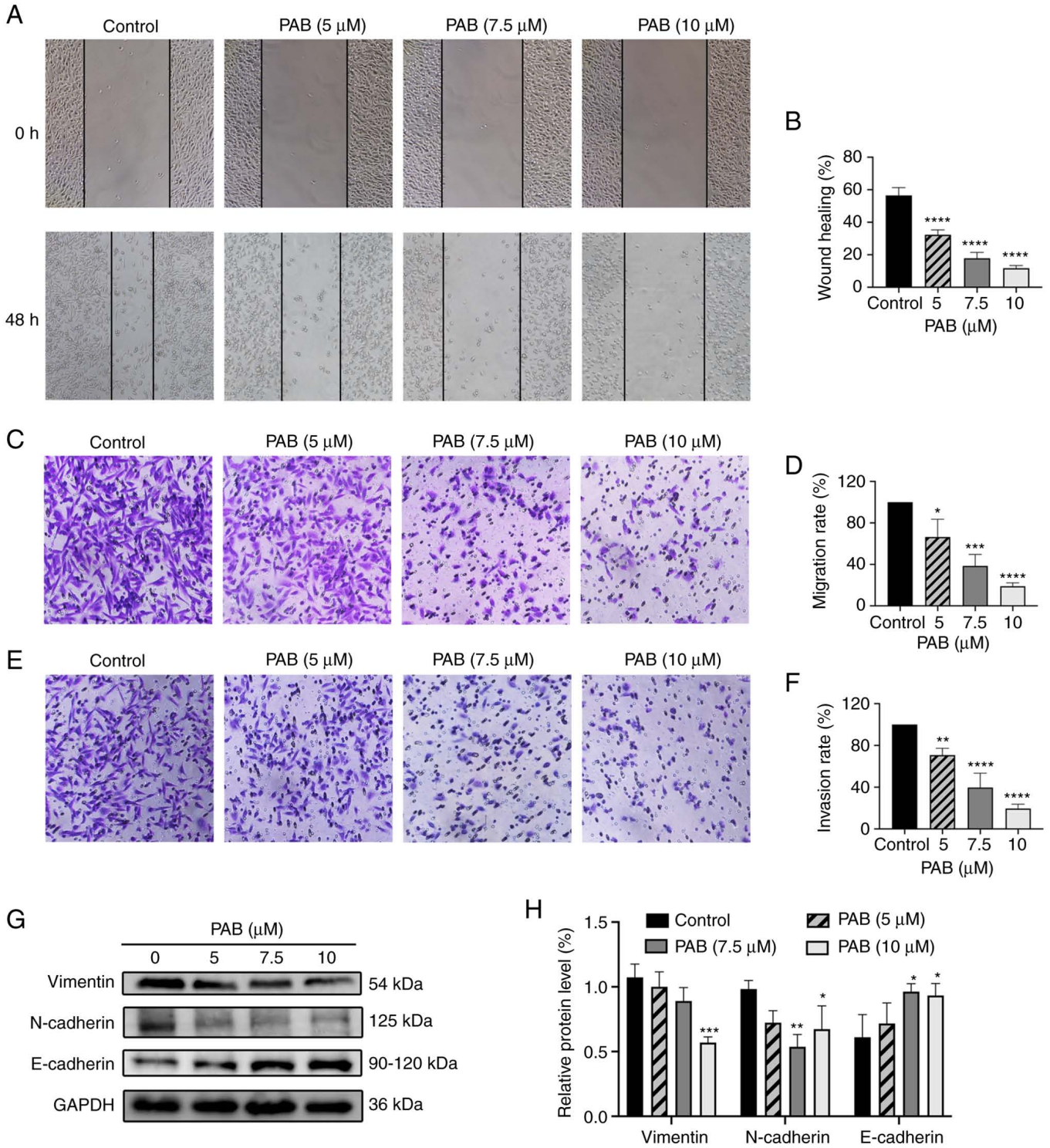

Figure 5. PAB suppresses MDA-MB-231 cells migration, invasion and epithelial-mesenchymal transition. (A) Wound healing assay (magnification, x200) and (B) quantitative analysis data. (C) Transwell migration assay (magnification, x100) was performed and (D) quantified to detect the migration ability of cells treated by PAB. (E) Transwell invasion assay (magnification, x100) was performed and (F) quantified to detect the invasion ability of cells treated by PAB. (G) Expression of markers for epithelial-mesenchymal transition in MDA-MB-231 cells with PAB treatment by western blotting. (H) Quantitative data of the relative protein expression. *P<0.05, **P<0.01, ***P<0.001, ****P<0.0001 vs. control. PAB, Pseudolaric acid B.

anti-apoptosis proteins Bcl-2 and Bcl-xl and increased the pro-apoptosis protein Bax. These results suggested that PAB induced apoptosis of MDA-MB-231 cells via the mitochondrial apoptosis pathway (Fig. S1).

The PI3K/AKT/mTOR signaling pathway, an important regulator of tumor proliferation, apoptosis, invasion and migration, is closely related to the expression of Bcl-2 family proteins in the mitochondrial apoptosis pathway (22). Western blotting showed that treatment of TNBC cells with PAB significantly decreased levels of PI3K (p110β), p-AKT and p-mTOR. Its apoptosis effect was also significantly elevated when combined with LY294002, a PI3K

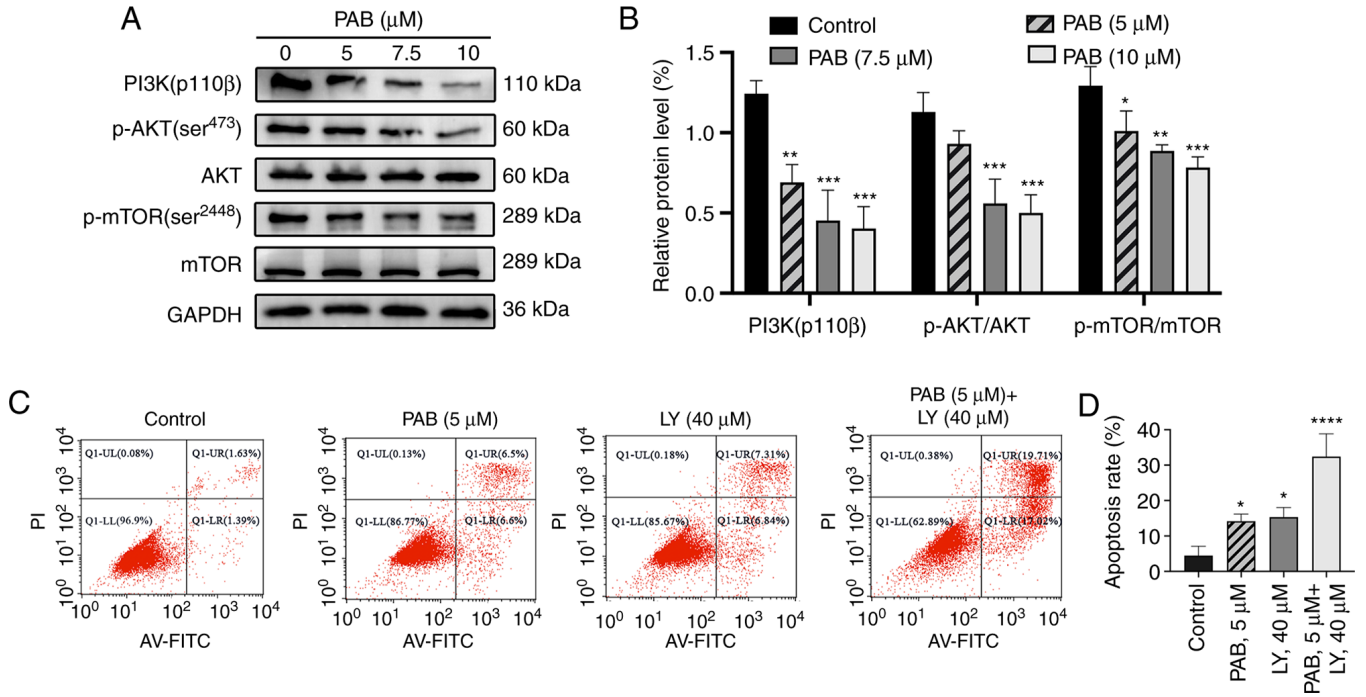

Figure 6. PAB inhibits the PI3K/mTOR/AKT signaling pathway. (A) MDA-MB-231 cells were exposed to the indicated doses of PAB for 48 h. The expression levels of PI3K, p-AKT (ser473), AKT, p-mTOR (ser3448) and mTOR were assessed by western blotting. (B) Quantitative data of the relative protein expression. (C) Cells were pretreated with PAB (5 μM), LY294002 (40 μM) or both for 48 h. Annexin V-FITC and PI staining were used to identify apoptosis rate, and (D) the data were analyzed by flow cytometry. *P<0.05, **P<0.01, ***P<0.001, ****P<0.0001 vs. control. PAB, Pseudolaric acid B; p-, phosphorylated.

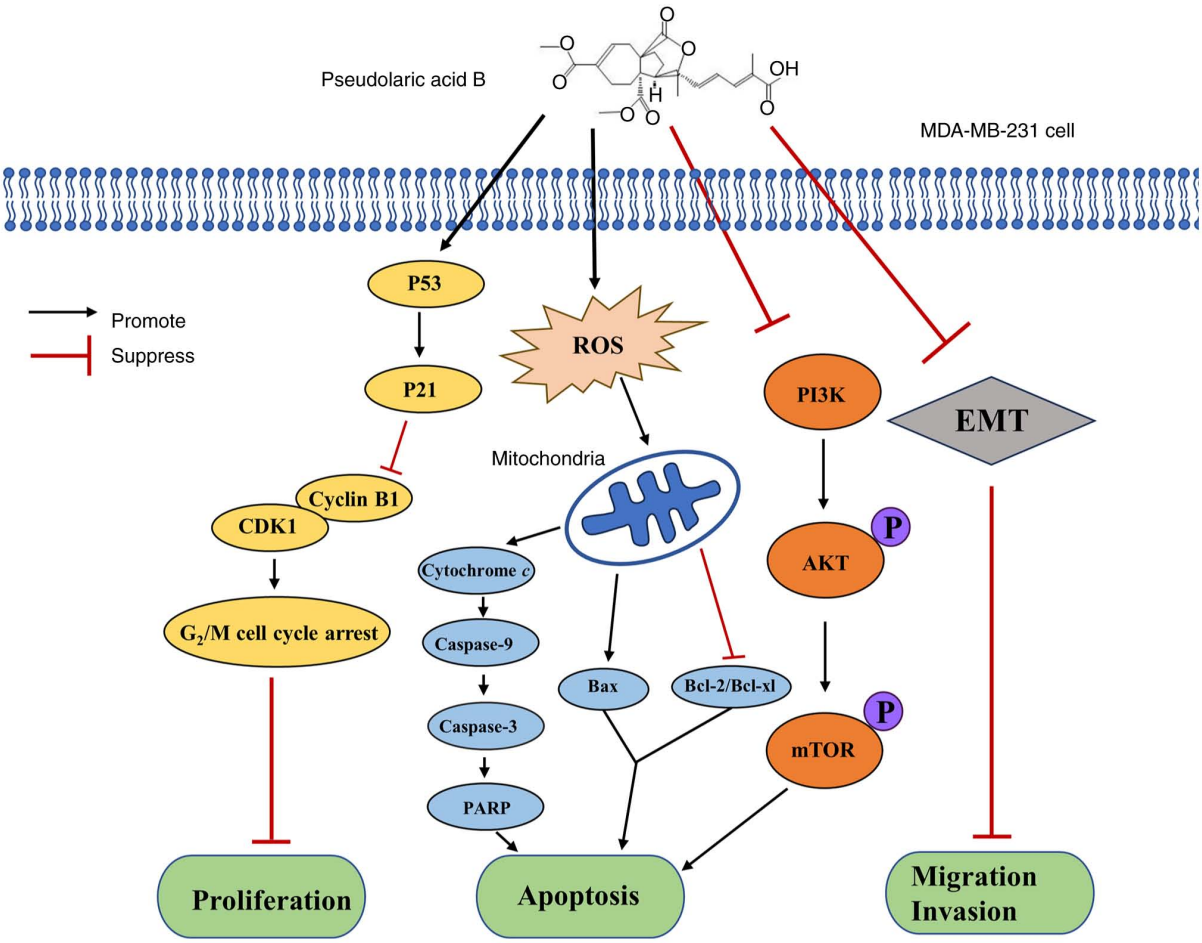

Figure 7. Plausible delivery mechanisms through which pseudolaric acid B exerts multiple anticancer activities through multiple targets in triple negative breast cancer. ROS, reactive oxygen species; EMT, epithelial-mesenchymal transition.

inhibitor. These data demonstrated that PI3K/AKT/mTOR signaling may be the target of PAB-induced apoptosis in MDA-MB-231 cells.

TNBC is the most aggressive and malignant type of breast cancer, and is more likely to develop lung and brain metastases (43-45). The present study revealed that EMT is critical for regulating the proliferation, invasion and metastasis of carcinoma cells (46). Activation of the EMT mechanism depends on loss of the epithelial marker E-cadherin and the upregulation of mesenchymal markers N-cadherin and vimentin, thereby prompting tumor cells through multiple steps in the process of invasion and metastasis (47,48). Results of the present wound-healing and Transwell assays suggested that PAB inhibited the ability of cells to migrate and invade. Further experiments demonstrated that it decreased the levels of N-cadherin and vimentin and increased the level of E-cadherin. These results suggested that EMT in MDA-MB-231 cells could be inhibited by PAB treatment.

There are several limitations and challenges to the present research. First, it was only verified that the mechanism of PAB-induced apoptosis in MDA-MB-231 cells was related to the mitochondrial apoptosis pathway, but it was not verified whether it was dependent on the mitochondrial apoptosis pathway. Second, the present study demonstrated that the PI3K/AKT/mTOR signaling pathway had a superpositioned effect on PAB-induced apoptosis, but the specific mechanism of action has not been clearly explored. Future studies will hopefully explore the specific role of PI3K/AKT/mTOR signaling pathway in PAB-induced apoptosis. Third, although the aim of the present study was to demonstrate how PAB plays an anticancer role in TNBC, the specific mechanism of PAB *in vivo* studies remains to be determined. In addition, a previous study has revealed that PAB-induced autophagy of breast cancer cells line MCF-7 inhibits apoptosis and promotes cell survival, which indicates that the combination of autophagy inhibitors may improve the anticancer effect of PAB (49).

In conclusion, the present results demonstrated that PAB exhibited anticancer effects against TNBC and that the mechanism was related to multiple pathways (Fig. 7). The present study revealed that PAB significantly inhibited the proliferative ability of MDA-MB-231 cells by arresting the cell at the G_2/M phase. The pro-apoptotic activity of PAB in TNBC was demonstrated through activation of the mitochondrial apoptosis pathway and inhibition of the PI3K/AKT/mTOR signaling pathway. PAB also demonstrated an anticancer effect on TNBC by inhibiting cell migration and invasion, through a mechanism related to the suppression of EMT. Overall, these results provided evidence that PAB exerted multiple anticancer activities through multiple targets in TNBC.

Acknowledgements

The group would like to thank Professor Caigang Liu from Shengjing Hospital Cancer Research Center (Shenyang, China) for the cell support. The group would like to thank Professor Yuxin Tong, Medical Research Center, Shengjing Hospital of China Medical University (Shenyang, China) for technical guidance.

Funding

This work was supported by a grant from the Science and Technology Project of Liaoning Province (grant no. 2014226033).

Availability of data and materials

The data used and/or analyzed during the present study are available from the corresponding author on reasonable request.

Authors' contributions

FY, SNC and KL designed the study and revised the manuscript. KY and JQW performed the experiments and drafted the manuscript together. All authors read and approved the final manuscript. KY and JQW confirm the authenticity of all the raw data.

Ethical approval and consent to participate

Not applicable.

Patient consent for publication

Not applicable.

Competing interests

The authors declare that they have no competing interests.

References

1. Sung H, Ferlay J, Siegel RL, Laversanne M, Soerjomataram I, Jemal A and Bray F: Global cancer statistics 2020: GLOBOCAN estimates of incidence and mortality worldwide for 36 cancers in 185 countries. CA Cancer J Clin 71: 209-249, 2021.
2. Yin L, Duan JJ, Bian XW and Yu SC: Triple-negative breast cancer molecular subtyping and treatment progress. Breast Cancer Res 22: 61, 2020.
3. Garrido-Castro AC, Lin NU and Polyak K: Insights into molecular classifications of triple-negative breast cancer: Improving patient selection for treatment. Cancer Discov 9: 176-198, 2019.
4. Lu J, Guan H, Wu D, Hu Z, Zhang H, Jiang H, Yu J, Zeng K, Li H, Zhang H, *et al*: Pseudolaric acid B ameliorates synovial inflammation and vessel formation by stabilizing PPARγ to inhibit NF-κB signalling pathway. J Cell Mol Med 25: 6664-6678, 2021.
5. Li Z, Yin H, Chen W, Jiang C, Hu J, Xue Y, Yao D, Peng Y and Hu X: Synergistic effect of pseudolaric Acid B with fluconazole against resistant isolates and biofilm of candida tropicalis. Infect Drug Resist 13: 2733-2743, 2020.
6. Miao ZH, Feng JM and Ding J: Newly discovered angiogenesis inhibitors and their mechanisms of action. Acta Pharmacol Sin 33: 1103-11, 2012.
7. Wei SF, He DH, Zhang SB, Lu Y, Ye X, Fan XZ, Wang H, Wang Q and Liu YQ: Identification of pseudolaric acid B as a novel Hedgehog pathway inhibitor in medulloblastoma. Biochem Pharmacol 190: 114593, 2021.
8. Mafu S, Karunanithi PS, Palazzo TA, Harrod BL, Rodriguez SM, Mollhoff IN, O'Brien TE, Tong S, Fiehn O, Tantillo DJ, *et al*: Biosynthesis of the microtubule-destabilizing diterpene pseudolaric acid B from golden larch involves an unusual diterpene synthase. Proc Natl Acad Sci USA 114: 974-979, 2017.
9. Zhang H, Li JC, Luo H, Zhao L, Zhang ZD and Shen XF: Pseudolaric acid B exhibits anti-cancer activity on human hepatocellular carcinoma through inhibition of multiple carcinogenic signaling pathways. Phytomedicine 59: 152759, 2019.

10. Wang D, Xin Y, Tian Y, Li W, Sun D and Yang Y: Pseudolaric acid B inhibits gastric cancer cell metastasis in vitro and in haematogenous dissemination model through PI3K/AKT, ERK1/2 and mitochondria-mediated apoptosis pathways. Exp Cell Res 352: 34-44, 2017.
11. Yao GD, Yang J, Li XX, Song XY, Hayashi T, Tashiro SI, Onodera S, Song SJ and Ikejima T: Blocking the utilization of glucose induces the switch from senescence to apoptosis in pseudolaric acid B-treated human lung cancer cells in vitro. Acta Pharmacol Sin 38: 1401-1411, 2017.
12. Jiang L, Wen C, He Q, Sun Y, Wang J, Lan X, Rohondia S, Dou QP, Shi X and Liu J: Pseudolaric acid B induces mitotic arrest and apoptosis in both imatinib-sensitive and -resistant chronic myeloid leukaemia cells. Eur J Pharmacol 876: 173064, 2020.
13. Hanahan D: Hallmarks of cancer: New dimensions. Cancer Discov 12: 31-46, 2022.
14. Jeong SY and Seol DW: The role of mitochondria in apoptosis. BMB Rep 41: 11-22, 2008.
15. Carneiro BA and El-Deiry WS: Targeting apoptosis in cancer therapy. Nat Rev Clin Oncol 17: 395-417, 2020.
16. Guan D, Li C, Lv X and Yang Y: Pseudolaric acid B inhibits PAX2 expression through Wnt signaling and induces BAX expression, therefore promoting apoptosis in HeLa cervical cancer cells. J Gynecol Oncol 30: e77, 2019.
17. Choi SJ, Ahn CH, Yang IH, Jin B, Lee WW, Kim JH, Ahn MH, Swarup N, Hong KO, Shin JA, *et al*: Pseudolaric Acid B induces growth inhibition and caspase-dependent apoptosis on head and neck cancer cell lines through death receptor 5. Molecules 24: 3715, 2019.
18. Wen C, Chen J, Zhang D, Wang H, Che J, Qin Q, He L, Cai Z, Lin M, Lou Q, *et al*: Pseudolaric acid B induces mitotic arrest and apoptosis in both 5-fluorouracil-sensitive and -resistant colorectal cancer cells. Cancer Lett 383: 295-308, 2016.
19. Polivka J Jr and Janku F: Molecular targets for cancer therapy in the PI3K/AKT/mTOR pathway. Pharmacol Ther 142: 164-175, 2014.
20. Bartholomeusz C and Gonzalez-Angulo AM: Targeting the PI3K signaling pathway in cancer therapy. Expert Opin Ther Targets 16: 121-130, 2012.
21. Claerhout S, Decraene D, Van Laethem A, Van Kelst S, Agostinis P and Garmyn M: AKT delays the early-activated apoptotic pathway in UVB-irradiated keratinocytes via BAD translocation. J Invest Dermatol 127: 429-438, 2007.
22. Quan JH, Cha GH, Zhou W, Chu JQ, Nishikawa Y and Lee YH: Involvement of PI 3 kinase/Akt-dependent Bad phosphorylation in Toxoplasma gondii-mediated inhibition of host cell apoptosis. Exp Parasitol 133: 462-471, 2013.
23. Fulda S: Synthetic lethality by co-targeting mitochondrial apoptosis and PI3K/Akt/mTOR signaling. Mitochondrion 19: 85-87, 2014.
24. Zuo A, Zhao P, Zheng Y, Hua H and Wang X: Tripterine inhibits proliferation, migration and invasion of breast cancer MDA-MB-231 cells by up-regulating microRNA-15a. Biol Chem 400: 1069-1078, 2019.
25. Yang W, Feng B, Meng Y, Wang J, Geng B, Cui Q, Zhang H, Yang Y and Yang J: FAM3C-YY1 axis is essential for TGFβ-promoted proliferation and migration of human breast cancer MDA-MB-231 cells via the activation of HSF1. J Cell Mol Med 23: 3464-3475, 2019.
26. Lou C, Xu X, Chen Y and Zhao H: Alisol A suppresses proliferation, migration, and invasion in human breast cancer MDA-MB-231 cells. Molecules 24: 3651, 2019.
27. Kheirandish-Rostami M, Roudkenar MH, Jahanian-Najafabadi A, Tomita K, Kuwahara Y, Sato T and Roushandeh AM: Mitochondrial characteristics contribute to proliferation and migration potency of MDA-MB-231 cancer cells and their response to cisplatin treatment. Life Sci 244: 117339, 2020.
28. Tohkayomatee R, Reabroi S, Tungmunnithum D, Parichatikanond W and Pinthong D: Andrographolide exhibits anticancer activity against breast cancer cells (MCF-7 and MDA-MB-231 cells) through suppressing cell proliferation and inducing cell apoptosis via inactivation of ER-α receptor and PI3K/AKT/mTOR signaling. Molecules 27: 3544, 2022.
29. Yu B, Yue DM, Shu LH, Li NJ and Wang JH: Pseudolaric acid B induces caspase-dependent cell death in human ovarian cancer cells. Oncol Rep 31: 849-857, 2014.
30. Wang D, Tian Y, Feng W, Zhao L, Zhao M, Liu J and Wang Q: Pseudolaric acid B induces endometrial cancer Ishikawa cell apoptosis and inhibits metastasis through AKT-GSK-3β and ERK1/2 signaling pathways. Anticancer Drugs 28: 603-612, 2017.
31. Li X, Zhao X, Song W, Tian Z, Yang L, Niu Q, Zhang Q, Xie M, Zhou B, Xu Y, *et al*: Pseudolaric Acid B inhibits proliferation, invasion and Epithelial-to-mesenchymal transition in human pancreatic cancer cell. Yonsei Med J 59: 20-27, 2018.
32. Matthews HK, Bertoli C and de Bruin RAM: Cell cycle control in cancer. Nat Rev Mol Cell Biol 23: 74-88, 2022.
33. Dong C, Wen S, Zhao S, Sun S, Zhao S, Dong W, Han P, Chen Q, Gong T, Chen W, *et al*: Salidroside inhibits reactive astrogliosis and glial scar formation in late cerebral ischemia via the Akt/GSK-3β pathway. Neurochem Res 46: 755-769, 2021.
34. Bao Y, Wu X, Jin X, Kanematsu A, Nojima M, Kakehi Y and Yamamoto S: Apigenin inhibits renal cell carcinoma cell proliferation through G2/M phase cell cycle arrest. Oncol Rep 47: 60, 2022.
35. He YC, He L, Khoshaba R, Lu FG, Cai C, Zhou FL, Liao DF and Cao D: Curcumin nicotinate selectively induces cancer cell apoptosis and cycle arrest through a P53-mediated mechanism. Molecules 24: 4179, 2019.
36. Ma K, Wang K, Zhou Y, Liu N, Guo W, Qi J, Hu Z, Su S, Tang P and Zhou X: Purified vitexin compound 1 serves as a promising antineoplastic agent in ovarian cancer. Front Oncol 11: 734708, 2021.
37. Xie B, Wang S, Jiang N and Li JJ: Cyclin B1/CDK1-regulated mitochondrial bioenergetics in cell cycle progression and tumor resistance. Cancer Lett 443: 56-66, 2019.
38. Fischer M, Quaas M, Steiner L and Engeland K: The p53-p21-DREAM-CDE/CHR pathway regulates G2/M cell cycle genes. Nucleic Acids Res 44: 164-174, 2016.
39. Engeland K: Cell cycle arrest through indirect transcriptional repression by p53: I have a DREAM. Cell Death Differ 25: 114-132, 2018.
40. Abate M, Festa A, Falco M, Lombardi A, Luce A, Grimaldi A, Zappavigna S, Sperlongano P, Irace C, Caraglia M and Misso G: Mitochondria as playmakers of apoptosis, autophagy and senescence. Semin Cell Dev Biol 98: 139-153, 2020.
41. Yang Y, Karakhanova S, Hartwig W, D'Haese JG, Philippov PP, Werner J and Bazhin AV: Mitochondria and mitochondrial ROS in cancer: Novel targets for anticancer therapy. J Cell Physiol 231: 2570-2581, 2016.
42. Cao K and Tait SWG: Apoptosis and cancer: Force awakens, phantom menace, or both? Int Rev Cell Mol Biol 337: 135-152, 2018.
43. Deepak KGK, Vempati R, Nagaraju GP, Dasari VR, S N, Rao DN and Malla RR: Tumor microenvironment: Challenges and opportunities in targeting metastasis of triple negative breast cancer. Pharmacol Res 153: 104683, 2020.
44. Hosonaga M, Saya H and Arima Y: Molecular and cellular mechanisms underlying brain metastasis of breast cancer. Cancer Metastasis Rev 39: 711-720, 2020.
45. Rakha EA and Chan S: Metastatic triple-negative breast cancer. Clin Oncol (R Coll Radiol) 23: 587-600, 2011.
46. Pastushenko I and Blanpain C: EMT transition states during tumor progression and metastasis. Trends Cell Biol 29: 212-226, 2019.
47. Zhang Y and Weinberg RA: Epithelial-to-mesenchymal transition in cancer: Complexity and opportunities. Front Med 12: 361-373, 2018.
48. Aiello NM and Kang Y: Context-dependent EMT programs in cancer metastasis. J Exp Med 216: 1016-1026, 2019.
49. Yu J, Chen C, Xu T, Yan M, Xue B, Wang Y, Liu C, Zhong T, Wang Z, Meng X, *et al*: Pseudolaric acid B activates autophagy in MCF-7 human breast cancer cells to prevent cell death. Oncol Lett 11: 1731-1737, 2016.